# Shoreline Change Assessment in Varosha, Famagusta, Cyprus: A Case Study of a Ghost Town Using Aerial Photographs and Very High-Resolution Satellite Data (1963–2024)

Christos Theocharidis [1,3*], Marinos Eliades [1], Kyriacos Themistocleous[1], Kyriacos Neocleous[1], Charalampos Kontoes [2], Diofantos Hadjimitsis [3,1]

[1] ERATOSTHENES Centre of Excellence, Department of Environment & Climate, Limassol 3012, Cyprus – christos.theocharidis@eratosthenes.org.cy
[2] National Observatory of Athens, Operational Unit BEYOND Centre for Earth Observation Research and Satellite Remote Sensing IAASARS/NOA, Athens, Greece – kontoes@noa.gr
3 Cyprus University of Technology, Department of Civil Engineering and Geomatics, Cyprus - d.hadjimitsis@cut.ac.cy

**Keywords:** Coastal erosion, DSAS, Varosha, MNDWI, Kalman, Remote Sensing

**Abstract**

Understanding and managing shoreline dynamics is crucial for the sustainability of coastal ecosystems. The natural forces combined with human activities and climate change continuously reshape our coastlines. This study provides a comprehensive and spatial accurate analysis of shoreline change along the Varosha coastline in Cyprus, covering the period from 1963 to 2024. Forecasts for 2034 and 2044 were conducted using the Kalman filter. Using aerial photographs and Very High-Resolution (VHR) satellite imagery, historical shorelines were mapped, and the erosion and accretion rates were quantified using the ArcGIS Pro and the Digital Shoreline Analysis System (DSAS). The findings revealed considerable spatial variations along the 6.4 km of the studied coastline. The northern and southern sections showed predominant erosional trends, with maximum erosion rates of -0.29 m/year, while the central region exhibited accretion, with maximum accretion rates of 0.43 m/year. This research emphasises the importance of continuous coastal monitoring and advanced geospatial analysis to inform sustainable management strategies. This rare case study enhances our understanding of natural coastal processes due to the absence of human interventions.

## 1. Introduction

Shoreline change assessment is a key aspect of coastal management, providing valuable insights into the dynamic interactions between terrestrial and marine ecosystems. Monitoring shorelines is essential for understanding the impacts of natural processes, such as erosion and sediment deposition (Al Ruheili and Boluwade, 2021), human activities and climate change (Toumasi et al., 2024). These examinations are vital for predicting future shoreline movements, informing sustainable development, and mitigating risks associated with coastal hazards (Griffiths et al., 2019; Palanisamy et al., 2024). The increasing frequency and intensity of coastal storms, sea-level rise, and human interventions underscores the need for shoreline monitoring. Accurate and continuous monitoring allows for identifying vulnerable areas, enabling timely and effective management strategies to protect coastal ecosystems and human infrastructure (Masria, 2024). Geospatial techniques and remote sensing have proven invaluable in tracking shoreline changes over time, especially through the use of High to VHR satellite data in recent decades. The high spatial detail of VHR imagery allows for the precise delineation of shoreline features, which is vital for identifying and quantifying small-scale changes in coastal morphology (Pampanoni et al., 2024; Randazzo et al., 2020; Smith et al., 2021). This level of detail is significant, especially in areas where erosion and accretion processes occur at fine spatial scales where lower-resolution satellite data cannot reveal these shifts (N. Apostolopoulos and G. Nikolakopoulos, 2020). In Europe, the significance of monitoring coastal changes, erosion and accretion is recognised through various legislative frameworks. The European Union's Directive 2014/89/EU established a framework for Maritime Spatial Planning (MSP), promoting an integrated approach to managing maritime and coastal areas such as Cyprus (Hadjimitsis et al., 2016) where numerous scientific studies have highlighted and supported with their actions the Cyprus's MSP (Agapiou et al., 2017; Danezis et al., 2020; EVAGOROU et al., n.d.; Hadjimitsis et al., 2015; Themistocleous et al., 2019). Despite the advancement of remote sensing science and the abundance of satellite data in recent years, only a limited number of studies focused on shoreline changes on the coasts of Cyprus. One notable study assessed the Coastal Vulnerability Index (CVI) along the Limassol coastline, evaluating the risks associated with human activities and climate change by exploiting various parameters to examine the shoreline shifts (Theocharidis et al., 2024). Another study examined the impact of climate change-induced hazards on tourist island beaches in Cyprus, assessing beach erosion due to storm events and sea-level rise, highlighting the importance of targeted coastal management strategies (Monioudi et al., 2023).

Additionally, Themistocleous (2023) conducted a study that exploited UAV data to monitor shoreline changes in Spyros Beach, located near Larnaca, demonstrating the effectiveness of UAV technology in capturing VHR data for coastal management. The studies above focused on areas with significant human activity and tourism. However, the case of the city of Varosha in the Famagusta (Ammochostos) district presents a unique opportunity to study shoreline dynamics in an abandoned area with minimal human intervention. To our knowledge, no studies have been conducted in this area to assess shoreline changes. Therefore, this study aims to contribute to existing knowledge by monitoring Varosha's shoreline dynamics for 1963–2024, utilising VHR satellite and aerial photograph data. The specific objectives are: 1) Analyse historical shoreline changes, 2) Identify and quantify the rates of erosion and accretion along the Varosha coastline, and 3) Contribute to the broader field of

* Corresponding author

coastal management by making predictions of the shoreline positions.

## 2. Study area

Varosha, located in the southern quarter of the city of Famagusta which is in the southeastern part of Cyprus is a coastal area that has remained uninhabited since mid-August 1974 due to the illegal Turkish military invasion of Cyprus (Pyla and Phokaides, 2020). Prior to its abandonment, Varosha was a prominent tourist destination renowned for its pristine beaches and vibrant economy (Holleran and Holleran, 2024). The forced evacuation of its residents has left the area in a state of repression, with infrastructure and buildings untouched for over five decades. This unique situation provides a rare opportunity to study natural coastal processes in the absence of human actions. The study area is characterised by sandy beaches and a generally low-lying topography, making it particularly susceptible to coastal dynamics such as erosion and sediment deposition. The studied coastline covers approximately 6.4 km and is located within a grid system comprising 17 shoreline grids, each measuring 1 × 1 km$^{2,}$ created to define the study area from the north side (A1 grid cell) to the south side (K2 grid cell) inside the borders of Varosha (Figure 1).

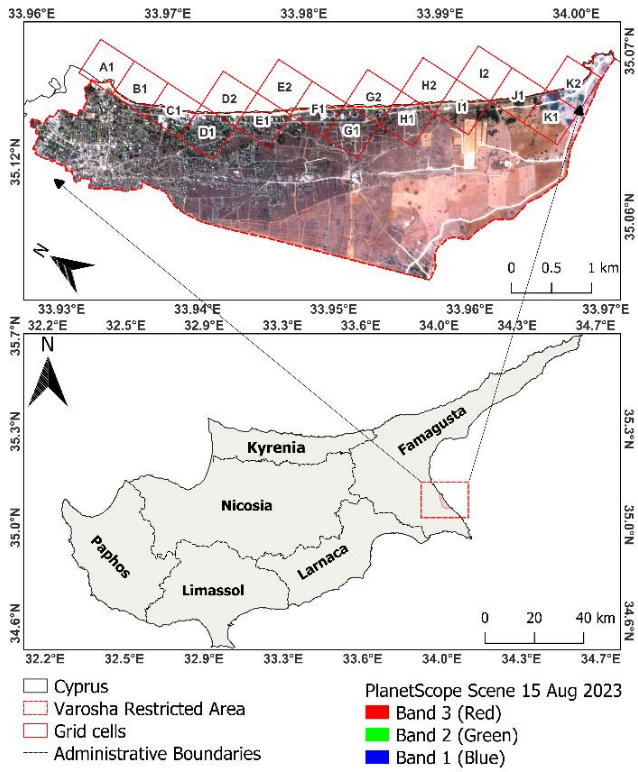


Figure 1. Study area.

## 3. Materials and methods

### 3.1 Data Collection

The study utilised a range of VHR satellite and aerial imagery to extract the historical shorelines in Varosha from 1963 to 2024, analysing 17 different shorelines in total. Table *1* provides information about the data and sources for the remote sensing used for the shoreline extraction and analysis. This study aimed to exploit imagery data captured primarily during the summer months to avoid interference from winter storms, which can temporarily alter the shoreline and create noise in the data. Focusing on the summer period, when weather conditions are more stable, and wave activity is lower, the study ensures more accurate detection of long–term shoreline positions and reduces the impact of seasonal storm events on the shoreline delineation process.

Table 1. Data and sources utilised in the study.

| Date | Remote Sensing data | Spatial Resolution | Source |
|---|---|---|---|
| 1963 | DLS Aerial Photo | 0.15 m | DLS portal |
| 27/07/1974 | Keyhole–9 | 0.8 m | USGS Earth Explorer |
| 24/10/2004 | OrbView 3 | 1 m | |
| 2009 | DLS Aerial Photo | 0.15 m | DLS portal |
| 28/07/2010 | RapidEye | 5 m | Planet |
| 10/06/2011 | | | |
| 24/07/2014 | | | |
| 20/05/2015 | | | |
| 23/08/2016 | PlanetScope | 3 m | |
| 27/07/2017 | | | |
| 13/07/2018 | | | |
| 08/07/2019 | | | |
| 25/06/2020 | SkySat | 0.5 m | |
| 07/09/2021 | | | |
| 22/09/2022 | | | |
| 20/08/2023 | | | |
| 01/03/2024 | | | |

### 3.2 Shoreline Extraction Method

#### 3.2.1 Aerial Photographs

Using the ArcGIS Pro software the ISO cluster unsupervised classification methods were applied to accurately delineate the shoreline from the two aerial photographs provided by DLS. This technique enabled shoreline features to be separated from other land cover types by clustering pixels based on spectral similarities. For this study, two distinct classes (Land and Water) were created to discriminate the shoreline effectively. While the ISO classification was generally effective, manual inspection and editing were conducted in certain areas to refine the Land–Water boundary, ensuring precise shoreline delineation.

#### 3.2.2 Optical Satellite Data

Regarding the optical satellite data, the Modified Normalised Difference Water Index (MNDWI) was exploited to enhance the Land–Water boundary, which is essential for accurate shoreline determination (Xu, 2006). Due to the lack of the Short-Wave InfraRed (SWIR) band in the exploited optical data, the Near-InfraRed (NIR) band was used as a substitute in the MNDWI formula. Despite the absence of the SWIR band, this adaptation performed an effective shoreline detection. The modified MNDWI formula is expressed as follows:

$$MNDWI = \frac{Green-NIR}{Green+NIR} \quad (1)$$

Green and NIR represent the reflectance of green and near-infrared bands, respectively. The value of MNDWI ranges from -1 to 1, where values above zero typically represent water pixels.

#### 3.2.3 Shoreline Change with DSAS

After extracting the shorelines from each dataset, the DSAS (v6.0.168) (Thieler et al., 2009) quantified the shoreline changes along the Varosha coastline. The shoreline of the year 1963 served as the actual baseline; then, the DSAS analysis utilised specific settings to ensure accurate shoreline change measurements. A 95% confidence interval provided reliable statistical results, while the transects were spaced every 25 meters with a smoothing distance of 150 meters to reduce noise without losing important shoreline details. An uncertainty threshold of 5 meters was chosen, reflecting the precision of the VHR data used in this study. Two primary metrics were calculated and highlighted in this analysis:

- Linear Regression (LRR): The LRR metric provides a consistent rate of change over the study period by fitting a linear regression line to all shoreline positions at each transect.
- Net Shoreline Movement (NSM): NSM is the distance between the earliest and the most recent shoreline positions for each transect, offering a straightforward view of the total shoreline change in meters.

#### 3.2.4 Shoreline Position Forecasting with QSCAT

Even though shoreline forecasting is a complicated procedure, it is invaluable information for decision-makers when dealing with long-term coastal management planning (Barzehkar et al., 2021; Farris et al., 2023; Goncalves et al., 2012). For shoreline forecasting, this study used the QGIS Shoreline Change Analysis Tool (QSCAT v0.4.1) – an open-source QGIS plugin (Facun et al., 2024). The Kalman filter was implemented according to the DSAS user guide (Himmelstoss et al., 2018), delivering an estimated shoreline position for 2034 and 2044 along each transect. For more detailed information about the Kalman Filter framework, please refer to Long and Plant, (2012).

## 4. Results

### 4.1 Linear Regression Rate (LRR)

The LRR was calculated for each transect to assess the rate of shoreline change in meters per year. Across the 255 transects along the Varosha coastline, the average LRR was 0.02 m/year. This minimal rate suggests a general trend of shoreline stability over the study period, with only a slight tendency toward accretion. This near–zero average can be misleading if viewed in isolation, as it masks significant spatial variations along the coastline. The maximum LRR is 0.43 m/year, and the minimum is -0.29 m/year, neither of which exceeds +1 or falls below -1. This range suggests that shoreline changes are moderate both in erosion and accretion, as classified by typical categories in the literature in order to have comparable results with similar studies(Bolanio et al., 2024; Hammar-Klose and Thieler, 2001; Mohamed, 2020). However, these kinds of interpretations are influenced by the specific LRR ranges used for classification, meaning that if a different scale were applied, such as one with tighter thresholds for high erosion and accretion, the same data might indicate higher severity in these areas. The analysis revealed notable results where 157 transects (61.56% of the total shoreline) had an LRR greater than zero, indicating accreted trends, covering a total shoreline length of 3.92 km. Four transects (1.55% of the total shoreline) have an LRR equal to zero, representing 100 meters of stable shoreline where no net change was observed. A total of 94 transects (36.86% of the total shoreline) displayed an LRR less than zero, implying erosional trends in 2.35 km of shoreline.

Moreover, based on Figure 1A, the northern (mainly in B1, C1 grid cells) and southern (mainly in K1, K2 grid cells) sections of the shoreline display erosional trends. In these areas, the LRR values are primarily negative, indicating shoreline retreat. On the contrary, the shoreline's central region, represented by grid cells D1–J1, faces accreted rates indicating sediment transportation. Further analysis of the results revealed that certain areas exhibited notable erosional and accreted patterns. The highest accretion rates were observed in grid cells A1 (Transect ID 3 – 0.43 m/year) and E2 (Transect ID 103 – 0.29 m/year). The most significant erosional trends were found in cells B1 (Transect ID 40 – -0.29 m/year), C1 (Transect ID 44 – -0.27 m/year), and K1 (Transect ID 237 – -0.23 m/year) highlighting areas with a continuous shoreline retreat (Figure *2*D).

### 4.2 Net Shoreline Movement (NSM)

NSM was estimated to provide a cumulative change in shoreline position for each transect from 1963 to 2024 (Figure *2*B). This extensive 61-year analysis gives a comprehensive understanding of shoreline dynamics for over six decades. The average NSM across all transects was 1.62 meters, suggesting an overall accretion trend. However, as with the LRR, using an average metric can be somewhat misleading when dealing with the complexity of shoreline behaviour since it fails to capture local shifts. The maximum negative NSM was -25.9 meters at transect ID 44 (Figure *2*C), revealing an area with a pronounced erosion (Figure *2* B1). On the other hand, the maximum positive NSM was 25.2 meters at transect ID 2 (Figure *2*C), showing significant accretion in this region (Figure *2* B2). Summarising the NSM results, there are 93 accreting transects with an average of +7.89 meters, while 162 eroding transects had an average NSM of -9.42 meters. Overall, 63.52% (4.05 km) of the transects showed positive NSM values, while 36.48% (2.32 km) displayed negative values (erosion).

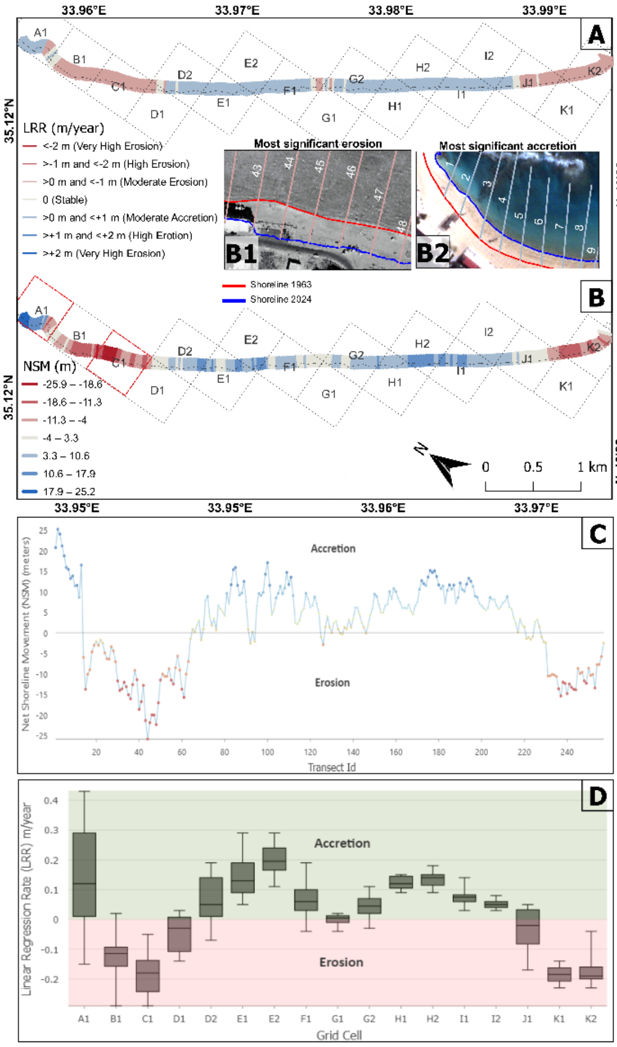


Figure 2. (A) Shoreline evolution of the study area by LRR (m/year) between 1963 and 2024. (B) Net Shoreline Movement of the studied coastline between 1963 and 2024. (B1) Most significant erosion. (B2) Most significant accretion. (C) Line chart of NSM per Transect ID. (D) Box plot chart of LRR per grid cell (The horizontal black line inside the box plots represents the median value).

### 4.3 Shoreline forecasting for 2034 and 2044

Predicting the shoreline position for 2034 and 2044, the forecasting statistics revealed significant trends along the Varosha coastline. However, due to limitations in the spatial coverage of the SkySat satellite in 2024, the shoreline predictions were explicitly implemented to grid cells A1 to J1. For the 2024–2034 period, the total change ranges between -8.23 and +3.15 meters, and the yearly rate varies between -0.82 to +0.31 m/year. The average total change for this period was negative, suggesting overall coastal erosion. Additionally, for 2024–2044, the total change exhibited a minimum of -10.56 m and a maximum of +4.29 m with a yearly rate range of -0.53– +0.43 m/year, reinforcing the erosion–dominated trend.

Analysing the forecasted shoreline positions, grid cell A1 was highlighted as having the most severe erosion among all grid cells, suggesting that this issue will intensify (Figure 3-B1–3) despite that grid cell A1 exhibited the highest accretion, demonstrating a varied pattern between erosion and accretion for this specific area. Furthermore, as mentioned earlier in sub-sections 4.1 and 4.2, the C1 grid cell faced the most extensive erosion (Figure 3 C1). Although a trend of accretion was observed in the southern section for the 2024–2034 period (Figure 3 C2), this pattern shifted to widespread erosion across most of the shoreline by 2044, as shown in Figure 3 C3. Furthermore, as presented earlier, grid cell E1 experienced the most notable accretion (Figure 3 D1). This trend is expected to persist through 2034 and 2044, with predictions highlighting E1 as the grid cell with the most significant accretion compared to the other grid cells Figure 3 D2–3).

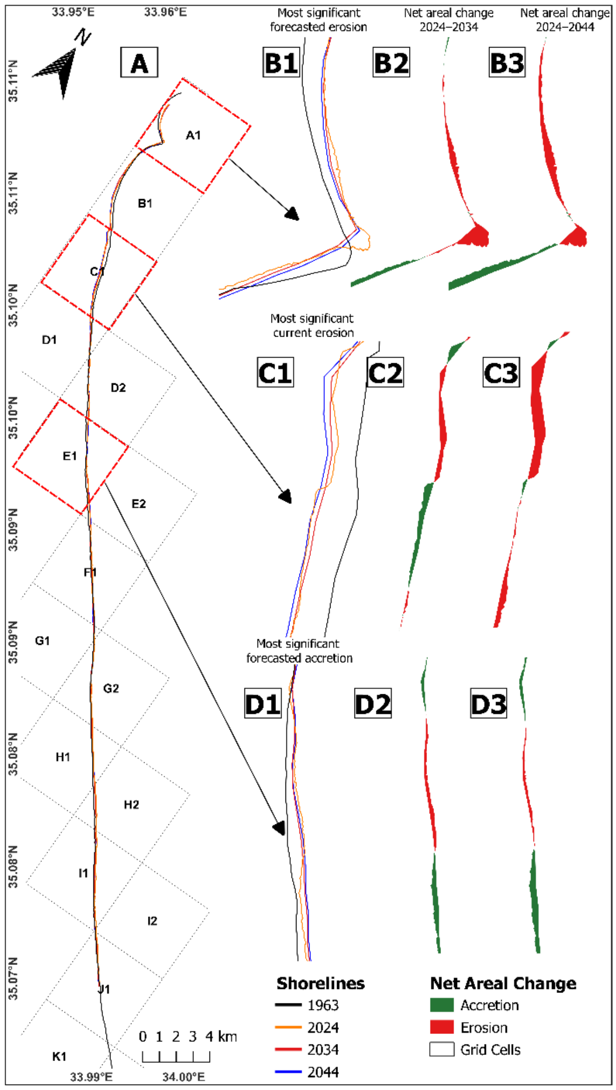


Figure 3. (A) Varosha coastline with the shorelines 1963, 2024, 2034 and 2044, (B1) Most significant forecasted erosion, (C1) Most significant current erosion, (D1) Most significant forecasted accretion (B2–D2) Net areal change for 2024–2034, (B3–D3) Net areal change for 2024–2044.

## 5. Discussion

The analysis of shoreline changes along the Varosha coastline from 1963 to 2024 revealed significant insights into this unique area's coastal dynamic. The results indicated a general stability trend with slight accretion but with notable spatial variations along the coastline. The observed accretion in the central section of the studied coastline suggests that combined sediment transportation and deposition could be influenced by the area's low-lying topography and the absence of tourists. These findings seem to align with similar studies conducted in Cyprus, which have also observed varying erosion and accretion rates (Monioudi et al., 2023; Theocharidis et al., 2024). However, it is essential to note that no similar studies specifically focused on the Varosha coastline, making it difficult to compare the study outcomes directly with those of other research. This lack of comparable studies is also evident when considering abandoned places like Varosha, where human intervention is minimal and natural processes dominate. According to the literature, only one study was identified that examined other abandoned places with similar dynamics. This research focused on coastal erosion in an abandoned mining settlement in Svalbard and employed software tools, such as ArcGIS Pro and DSAS, to calculate the same metrics as the LRR and NSM used in our study (Nicu et al., 2020). Overall, both periods demonstrated an erosion-dominated trend, with the 2024-2044 period reflecting more extreme changes in terms of total erosion and accretion compared to the 2024-2034 period. The differences in yearly rates also highlighted variable dynamics affecting different sections of the coastline over time.

## 6. Conclusions

This study examined shoreline changes in Varosha in the district of Famagusta in Cyprus for 61 years (1963–2024). Integrating aerial photographs and VHR satellite data, the research aimed to analyse historical shoreline positions, quantify the erosion and accretion rates and contribute to the broader field of coastal management, offering a unique case study of shoreline dynamics in an abandoned urban area. The findings revealed that the Varosha coastline has experienced both erosion and accretion with significant spatial variations along different sections of the shoreline. The northern and southern sections showed predominant erosional trends, while the central section of the studied coastline exhibited accretion. The study also forecasted future shoreline positions for 2034 and 2044, indicating an overall erosion–dominated trend, with specific areas expected to face more severe changes. The buildings located on the coastline can also be affected by erosion as they are exposed to waves, saltwater, and high winds, which results in damage to the building's foundations, structure, and materials, as well as corrosion in metal materials. This research highlights the importance of continuous monitoring and applying advanced geospatial technologies in understanding and managing coastal dynamics. This unique opportunity in the Varosha case, with no human interventions over the past five decades, provided valuable information on natural coastal processes, which can inform sustainable coastal management strategies in similar environments.

## Acknowledgements

The authors acknowledge the 'EXCELSIOR': ERATOSTHENES: Excellence Research Centre for Earth Surveillance and Space-Based Monitoring of the Environment H2020 Widespread Teaming project (www.excelsior2020.eu). The 'EXCELSIOR' project has received funding from the European Union's Horizon 2020 research and innovation programme under Grant Agreement No 857510, from the Government of the Republic of Cyprus through the Directorate General for the European Programmes, Coordination and Development and the Cyprus University of Technology.

## References

Agapiou, A., Lysandrou, V., Hadjimitsis, D.G., 2017. The Cyprus coastal heritage landscapes within Marine Spatial Planning process. J. Cult. Herit. 23, 28–36. https://doi.org/10.1016/j.culher.2016.02.016

Al Ruheili, A.M., Boluwade, A., 2021. Quantifying Coastal Shoreline Erosion Due to Climatic Extremes Using Remote-Sensed Estimates from Sentinel-2A Data. Environ. Process. 8, 1121–1140. https://doi.org/10.1007/s40710-021-00522-2

Barzehkar, M., Parnell, K.E., Soomere, T., Dragovich, D., Engström, J., 2021. Decision support tools, systems and indices for sustainable coastal planning and management: A review. Ocean Coast. Manag. 212, 105813. https://doi.org/10.1016/j.ocecoaman.2021.105813

Bolanio, K.P., Digal, L.G.S., Estilo, H.J.R., Seronay, R.A., 2024. SPATIO-TEMPORAL SCALES OF LAND COVER AND SHORELINE DYNAMICS IN BANAYBANAY, DAVAO ORIENTAL, PHILIPPINES USING AVAILABLE OPTICAL SATELLITE IMAGERY. Int. Arch. Photogramm. Remote Sens. Spat. Inf. Sci. 48, 61–67.

Danezis, C., Nikolaidis, M., Mettas, C., Hadjimitsis, D.G., Kokosis, G., Kleanthous, C., 2020. Establishing an Integrated Permanent Sea-Level Monitoring Infrastructure towards the Implementation of Maritime Spatial Planning in Cyprus. J. Mar. Sci. Eng. 8, 861. https://doi.org/10.3390/jmse8110861

EVAGOROU, E., METTAS, C., TZOUVARAS, M., LOULLI, E., PRODROMOU, M., PAPOUTSA, C., THEMISTOCLEOUS, K., DANEZIS, C., PEKRI, M., KYRIAKIDIS, P., n.d. Implementation of Maritime Spatial Planning (MSP) in Cyprus focusing on the European MSPs' good practices.

Facun, L.P., Sta. Maria, M.Y., Ducao, R., Clemente, J.J., Carmelo, E.M., Maon, A., Malaya, A.R., Cuison, F., Siringan, F., 2024. QGIS Shoreline Change Analysis Tool (QSCAT): A fast, open-source shoreline change analysis plugin for QGIS.

Farris, A.S., Long, J.W., Himmelstoss, E.A., 2023. Accuracy of shoreline forecasting using sparse data. Ocean Coast. Manag. 239, 106621. https://doi.org/10.1016/j.ocecoaman.2023.106621

Goncalves, R.M., Awange, J.L., Krueger, C.P., Heck, B., Coelho, L. dos S., 2012. A comparison between three short-term shoreline prediction models. Ocean Coast. Manag. 69, 102–110. https://doi.org/10.1016/j.ocecoaman.2012.07.024

Griffiths, D., House, C., Rangel-Buitrago, N., Thomas, T., 2019. An assessment of areal and transect-based historic shoreline changes in the context of coastal planning. J. Coast. Conserv. 23, 315–330. https://doi.org/10.1007/s11852-018-0661-6

Hadjimitsis, D., Agapiou, A., Themistocleous, K., Mettas, C., Evagorou, E., Soulis, G., Xagoraris, Z., Pilikou, M., Aliouris, K., Ioannou, N., 2016. Maritime Spatial Planning in Cyprus. Open Geosci. 8. https://doi.org/10.1515/geo-2016-0061

Hadjimitsis, D., Agapiou, A., Themistocleous, K., Xagoraris, Z., Soulis, G., Mettas, C., Evagorou, E. 1, Aliouris, K., Ioannou, N., Kokkosis, G., 2015. Development of Web-GIS platform for implementing Marine Spatial Planning in Cyprus, in: Proceedings of the 14th International Conference on Environmental Science and Technology Athens, Greece. pp. 3–5.

Hammar-Klose, E.S., Thieler, E.R., 2001. Coastal vulnerability to sea-level rise: a preliminary database for the US Atlantic, Pacific, and Gulf of Mexico coasts. US Geological Survey,.

Himmelstoss, E.A., Henderson, R.E., Kratzmann, M.G., Farris, A.S., 2018. Digital Shoreline Analysis System (DSAS) version 5.0 user guide, Open-File Report. https://doi.org/10.3133/ofr20181179

Holleran, M., Holleran, S., 2024. Resisting dark tourism: Northern Cyprus's 'ghost city' of Varosha. City 1–13. https://doi.org/10.1080/13604813.2024.2356368

Long, J.W., Plant, N.G., 2012. Extended Kalman Filter framework for forecasting shoreline evolution. Geophys. Res. Lett. 39. https://doi.org/10.1029/2012GL052180

Masria, A., 2024. Bridging coastal challenges: The role of remote sensing and future research. Reg. Stud. Mar. Sci. 73, 103502. https://doi.org/10.1016/j.rsma.2024.103502

Mohamed, S.A., 2020. Coastal vulnerability assessment using GIS-Based multicriteria analysis of Alexandria-northwestern Nile Delta, Egypt. J. African Earth Sci. 163, 103751. https://doi.org/10.1016/j.jafrearsci.2020.103751

Monioudi, I.N., Velegrakis, A.F., Chatzistratis, D., Vousdoukas, M.I., Savva, C., Wang, D., Bove, G., Mentaschi, L., Paprotny, D., Morales-Nápoles, O., Chatzipavlis, A.E., Hasiotis, T., Manoutsoglou, E., 2023. Climate change - induced hazards on touristic island beaches: Cyprus, Eastern Mediterranean. Front. Mar. Sci. 10. https://doi.org/10.3389/fmars.2023.1188896

N. Apostolopoulos, D., G. Nikolakopoulos, K., 2020. Assessment and Quantification of the Accuracy of Low- and High-Resolution Remote Sensing Data for Shoreline Monitoring. ISPRS Int. J. Geo-Information 9, 391. https://doi.org/10.3390/ijgi9060391

Nicu, I.C., Stalsberg, K., Rubensdotter, L., Martens, V.V., Flyen, A.-C., 2020. Coastal Erosion Affecting Cultural Heritage in Svalbard. A Case Study in Hiorthhamn (Adventfjorden)—An Abandoned Mining Settlement. Sustainability 12, 2306. https://doi.org/10.3390/su12062306

Palanisamy, P., Sivakumar, V., Velusamy, P., Natarajan, L., 2024. Spatio-temporal analysis of shoreline changes and future forecast using remote sensing, GIS and kalman filter model: A case study of Rio de Janeiro, Brazil. J. South Am. Earth Sci. 133, 104701. https://doi.org/10.1016/j.jsames.2023.104701

Pampanoni, V., Fascetti, F., Cenci, L., Laneve, G., Santella, C., Boccia, V., 2024. Analysing the Relationship between Spatial Resolution, Sharpness and Signal-to-Noise Ratio of Very High Resolution Satellite Imagery Using an Automatic Edge Method. Remote Sens. 16, 1041. https://doi.org/10.3390/rs16061041

Pyla, P., Phokaides, P., 2020. "Dark and Dirty" Histories of Leisure and Architecture: Varosha's Past and Future. Archit. Theory Rev. 24, 27–45. https://doi.org/10.1080/13264826.2020.1753282

Randazzo, G., Barreca, G., Cascio, M., Crupi, A., Fontana, M., Gregorio, F., Lanza, S., Muzirafuti, A., 2020. Analysis of Very High Spatial Resolution Images for Automatic Shoreline Extraction and Satellite-Derived Bathymetry Mapping. Geosciences 10, 172. https://doi.org/10.3390/geosciences10050172

Smith, K.E.L., Terrano, J.F., Pitchford, J.L., Archer, M.J., 2021. Coastal Wetland Shoreline Change Monitoring: A Comparison of Shorelines from High-Resolution WorldView Satellite Imagery, Aerial Imagery, and Field Surveys. Remote Sens. 13, 3030. https://doi.org/10.3390/rs13153030

Themistocleous, K., 2023. Identification and forecasting of coastal erosion using aerial and UAV images, in: Themistocleous, K., Michaelides, S., Hadjimitsis, D.G., Papadavid, G. (Eds.), Ninth International Conference on Remote Sensing and Geoinformation of the Environment (RSCy2023). SPIE, p. 78. https://doi.org/10.1117/12.2683057

Themistocleous, K., Mettas, C., Evagorou, E., Hadjimitsis, D.G., 2019. The use of satellite remote sensing and UAV for the mapping of coastal areas for the use of marine spatial planning, in: Schulz, K., Nikolakopoulos, K.G., Michel, U. (Eds.), Earth Resources and Environmental Remote Sensing/GIS Applications X. SPIE, p. 36. https://doi.org/10.1117/12.2533064

Theocharidis, C., Doukanari, M., Kalogirou, E., Christofi, D., Mettas, C., Kontoes, C., Hadjimitsis, D., Argyriou, A. V., Eliades, M., 2024. Coastal Vulnerability Index (CVI) Assessment: Evaluating Risks Associated with Human-Made Activities along the Limassol Coastline, Cyprus. Remote Sens. 16, 3688. https://doi.org/10.3390/rs16193688

Thieler, E.R., Himmelstoss, E.A., Zichichi, J.L., Ergul, A., 2009. The Digital Shoreline Analysis System (DSAS) Version 4.0 - An ArcGIS extension for calculating shoreline change, Open-File Report. https://doi.org/10.3133/ofr20081278

Toumasi, P., Petropoulos, G.P., Detsikas, S.E., Kalogeropoulos, K., Tselos, N.G., 2024. Coastal Vulnerability Impact Assessment under Climate Change in the Arctic Coasts of Tromsø, Norway. Earth 5, 640–653. https://doi.org/10.3390/earth5040033

Xu, H., 2006. Modification of normalised difference water index (NDWI) to enhance open water features in remotely sensed imagery. Int. J. Remote Sens. 27, 3025–3033.